AJNR

MR Imaging of Head Trauma: Review of the Distribution and Radiopathologic Features of Traumatic Lesions

Lindell R. Gentry, John C. Godersky and Brad Thompson

AJNR Am J Neuroradiol 1988, 9 (1) 101-110
http://www.ajnr.org/content/9/1/101

This information is current as of August 22, 2025.

MR Imaging of Head Trauma:
Review of the Distribution and Radiopathologic Features of Traumatic Lesions

Lindell R. Gentry[1,2]
John C. Godersky[3]
Brad Thompson[1]

The distribution and extent of traumatic lesions were prospectively evaluated with MR imaging in 40 patients with closed head injuries. Primary intraaxial lesions were classified according to their distinctive topographical distribution within the brain and were of four main types: (1) diffuse axonal injury (48.2%), (2) cortical contusion (43.7%), (3) subcortical gray-matter injury (4.5%), and (4) primary brainstem injury (3.6%). Diffuse axonal injury most commonly involved the white matter of the frontal and temporal lobes, the body and splenium of the corpus callosum, and the corona radiata. Cortical contusions most frequently involved the inferior, lateral, and anterior aspects of the frontal and temporal lobes. Primary brainstem lesions were most commonly seen in the dorsolateral aspects of the rostral brainstem. The pattern and distribution of primary lesions seen by MR were compared with those expected from previous pathologic studies and found to be quite similar. Our data and review of the literature would also indicate that MR detects a more complete spectrum of traumatic lesions than does CT. Secondary forms of injury (territorial arterial infarction, pressure necrosis from increased intracranial pressure, cerebral herniation, secondary brainstem injury) were also visible by MR in some cases. The level of consciousness was most impaired in patients with primary brainstem injury, followed by those with widespread diffuse axonal injury and subcortical gray-matter injury. The best MR imaging planes, pulse sequences, and imaging strategies for evaluating and classifying traumatic lesions were evaluated, and the mechanisms by which traumatic stresses result in injury were reviewed.

MR was found to be superior to CT and to be very effective in the detection of traumatic head lesions and some secondary forms of injury. While T2-weighted images were most useful for lesion detection, T1-weighted images proved to be most useful for anatomic localization and classification.

This article appears in the January/February 1988 issue of *AJNR* and the March 1988 issue of *AJR*.

Received February 18, 1987; accepted after revision July 23, 1987.

Presented at the Symposium Neuroradiologicum, Stockholm, June 1986.

[1] Department of Radiology, University of Iowa Hospitals and Clinics, Iowa City, IA 52242.

[2] Present address: Department of Radiology, University of Wisconsin Hospital and Clinics, 600 Highland Dr., Madison, WI 53792. Address reprint requests to L. R. Gentry.

[3] Department of Surgery, Division of Neurosurgery, University of Iowa Hospital and Clinics, Iowa City, IA 52242.

***AJNR* 9:101–110, January/February 1988**
0195–6108/88/0901–0101
© American Society of Neuroradiology

In the last decade CT has played a critical role in the diagnostic evaluation of patients with closed head trauma, providing an accurate means of diagnosing potentially reversible intracranial hematomas [1–10]. Despite fulfilling this important role, CT has been less helpful in the detection and characterization of many types of traumatic lesions. It is apparent from pathologic studies that CT underestimates the severity of many forms of cerebral injury such as primary brainstem injury, nonhemorrhagic cortical contusion, and diffuse axonal injury [3, 5, 10–18]. Although autopsy studies have been helpful in characterizing the distribution and morphology of these lesions, they only reflect the nature of the disease in the most severely injured patients.

Since CT cannot accurately assess the full spectrum of lesions in patients, it has not been possible to develop clinically useful CT imaging criteria for classifying and staging the severity of cranial trauma [10, 13, 16–18]. MR, however, has been shown to be highly sensitive in detecting both hemorrhagic and nonhemorrhagic lesions [16]. With this new method, it should now be possible to accurately identify all types of traumatic lesions, classify them, and stage their extent in the living patient.

The purpose of this study was to determine the ability of MR to prospectively

identify and characterize the traumatic intraaxial lesions found in 40 patients with closed head trauma by using a simple anatomic and topographic method of classification. The location, frequency, and distribution of all visualized lesions were compared with that expected from postmortem and animal studies. The best imaging planes and pulse sequences for evaluating each category of traumatic lesion were assessed. We also reviewed the mechanisms by which traumatic stresses result in cerebral injury.

Subjects and Methods

A prospective MR study of 40 patients with acute closed head trauma was initiated after approval of the protocol by our hospitals' institutional review board. A more complete description of the study methodology is provided in the first article in this two-part report [16]. The ages of the patients ranged from 1 month to 82 years (mean, 26.6 years). The severity of injury, as measured by the admission Glascow Coma Scale (GCS), varied from 3 to 14 (mean, 9.8). MR scans were obtained as soon as possible after injury, unless the patients were medically or neurologically unstable. Twelve patients were examined with MR while being mechanically ventilated with a nonferromagnetic fluidic ventilator, as described by Dunn et al. [19].

Contiguous nonenhanced 8-mm CT scans were obtained in all patients within the first 24 hr of admission with a fourth-generation scanner.* MR scans were obtained with a 0.5-T system.† Contiguous 10-mm scans were obtained by using an interleaved multislice technique with two-dimensional Fourier reconstruction. Both T1- and T2-weighted pulse sequences were used in most patients. T2-weighted images were obtained by using a spin-echo sequence with a repetition time (TR) of 2300–2900 msec and echo time (TE) of 80–120 msec. T1-weighted images were obtained with either an inversion-recovery sequence with TR = 2000–2300 msec and inversion time (TI) of 500–600 msec or a spin-echo sequence with TR = 400–1000 msec, TE = 25–40 msec. Thirty-four patients were examined with two or more imaging planes, while six were studied with only one plane of imaging. Thirty-nine patients were studied in the transverse plane, while 31 and five patients, respectively, were studied in the coronal and sagittal planes.

An attempt was made to differentiate *primary* lesions (resulting from the initial traumatic force) from *secondary* ones (caused by diffuse brain swelling and edema, brain displacement and herniation, delayed hemorrhage, cerebral infarction, diffuse hypoxic injury) (Table 1) [11–13]. In many cases distinction between primary and secondary lesions was difficult. For purposes of statistical analysis, however, all focal abnormalities that were not obviously secondary in nature were classified as primary lesions. Primary intracranial lesions were classified according to the method outlined in Table 1. Primary intraaxial lesions were further subclassified by their location: (1) diffuse axonal injury (white-matter "shear" injury) (Figs. 1 and 2), (2) cortical contusion (Figs. 1–4), (3) subcortical gray-matter injury (Fig. 4), and (4) primary brainstem injury (Fig. 5) [16].

For statistical purposes, two MR criteria were used to classify a lesion as hemorrhagic. On T1-weighted scans, the shortening of the T1 relaxation time by methemoglobin within the hematoma had to be of sufficient degree that the hematoma was at least partially hyperintense relative to white matter. On T2-weighted images, we required evidence of central hypointensity (relative to brain parenchyma) within the hematoma. As described by Gomori et al. [20], the central hypointensity appears to be secondary to preferential T2 proton relaxation enhancement caused by either deoxyhemoglobin or methemoglobin within intact RBCs.

The MR and CT examinations were initially analyzed separately and then compared to determine the relative sensitivities of the imaging studies. These data constitute the substance of an accompanying report [16]. The frequency, anatomic distribution, and extent of all the major types of primary traumatic lesions were assessed on the MR images and compared with that expected from postmortem and animal studies [3, 11–15, 17, 21–30] to determine their conformity with previously hypothesized mechanopathologic theories of injury. The best MR imaging planes, pulse sequences and imaging strategies were determined from analysis of the data.

TABLE 1: Classification of Traumatic Intracranial Lesions

Types and Locations of Lesions
Primary lesions:
Intraaxial:
Diffuse axonal injury
Cortical contusion
Subcortical gray-matter injury
Primary brainstem injury
Extraaxial hematomas:
Subdural
Epidural
Diffuse hemorrhage:
Subarachnoid
Intraventricular
Secondary lesions:
Pressure necrosis (secondary to brain displacement and herniation)
Territorial arterial infarction
Diffuse hypoxic injury
Diffuse brain swelling
Boundary and terminal zone infarction
Other (e.g., fatty embolism, secondary hemorrhage, infection)

Classification, Characterization, and Localization of Primary Traumatic Lesions

Diffuse Axonal Injury

The most common type of primary lesion identified in this series was diffuse axonal injury [11, 14–17, 21–28]. Lesions classified in this category had to spare the overlying cortex and be localized to the white matter or gray/white-matter interface (corticomedullary junction). Diffuse axonal injury typically was characterized by diffuse, small, focal abnormalities limited to white-matter tracts. These lesions constituted 48.2% of all traumatic lesions in this series (Table 2) (Figs. 1 and 2). When present they tended to be multiple, with 50.3% of lesions found in the 15 patients with the most severe initial impairment of consciousness. Although most of the lesions were nonhemorrhagic, 18.8% did contain small central foci of blood. Hemorrhage within diffuse axonal lesions occurred more often in those portions of the white matter with the greatest vascularity. While 25.0% of capsular and 19.7% of lobar white-matter lesions were hemorrhagic, only 10.7% of the diffuse axonal lesions in the less vascular corona radiata contained blood. The size of diffuse axonal lesions ranged from 5 to 15 mm and varied with location. Peripheral lesions tended to be smaller than central ones. The shape of the lesions was usually ovoid to elliptical with the long axis parallel to the direction of the fiber bundles (Figs. 1 and 2). They were typically found near the corticomedullary interface of the lobar

* Picker 600 and 1200 scanners, Picker International, Highland Heights, OH.
† Picker International, Highland Heights, OH.

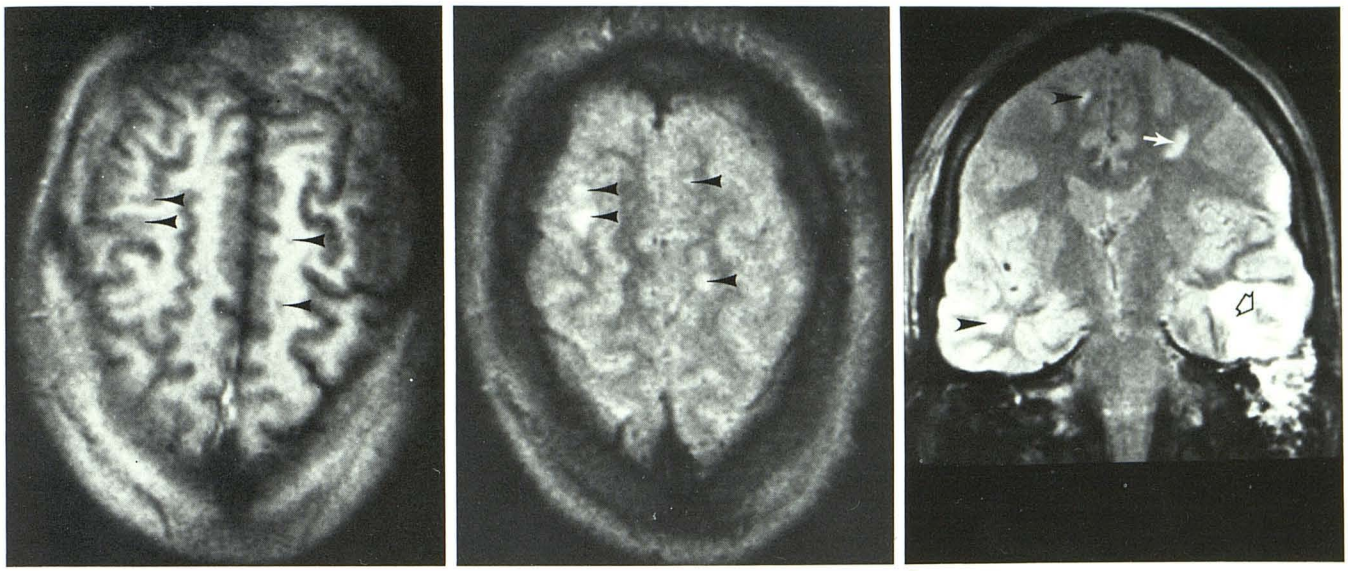

Fig. 1.—25-year-old man 4 days after trauma. Axial T1-weighted inversion-recovery (TR = 2100 msec, TI = 600 msec) MR image (*A*) and axial (*B*) and coronal (*C*) T2-weighted spin-echo (TR = 2300 msec, TE = 80 msec) MR images. Multiple bilateral diffuse axonal lesions are at corticomedullary interface of frontal, parietal, and temporal lobes (*arrowheads*).

***C*, Coronal T2-weighted MR image aids in lesion classification by helping to confirm that diffuse axonal lesions are within white matter, rather than at depths of cortical sulci. Note sparing of overlying cortex. Larger ovoid diffuse axonal lesion (*solid arrow*) is present in corona radiata, oriented parallel to direction of fiber tracts. Typical cortical contusion is present in inferolateral aspect of temporal lobe (*open arrow*). Note.—Contusion is cortically based and displaces uninvolved white matter. Peripheral zone of nonhemorrhagic injury is around central hypointensity of hematoma (*open arrow*). Hypointensity of acute hematoma at 0.5 T is always less pronounced than at higher field strengths.**

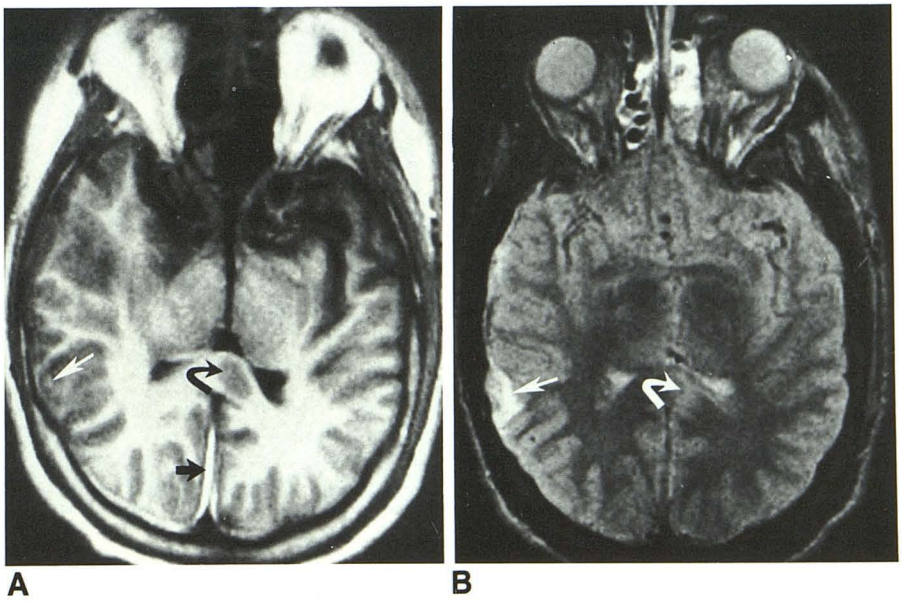

Fig. 2.—35-year-old man 4 days after trauma. Axial T1-weighted inversion-recovery (TR = 2100 msec, TI = 600 msec) MR image (*A*) and axial T2-weighted spin-echo (TR = 2300 msec, TE = 80 msec) MR image (*B*) show large ovoid diffuse axonal lesion in splenium of corpus callosum (*curved arrows*). Callosal diffuse axonal lesions were most common in this location. Also noted is small temporal lobe cortical contusion (*straight arrows*) that is difficult to identify on T1-weighted image (*A*). Four-day-old interhemispheric subdural lesion (*black arrow* in *A*) is more clearly seen at this age on T1-weighted scan.

white matter or in the large white-matter fiber bundles (corona radiata, corpus callosum, internal capsule).

The majority of the diffuse axonal lesions (50.3%) were located adjacent to the gray matter in the lobar white matter. The frontal and temporal lobes were involved most commonly, with 48.0% and 30.7% of lesions, respectively, located in these regions (Table 2). The parietal lobes, occipital lobes, and cerebellum were involved less often. The lesions of the frontal white matter were distributed equally along the superior, inferior, and lateral aspects of this lobe. White-matter lesions in the temporal lobe tended to lie adjacent to the temporal horn of the lateral ventricle (Fig. 1).

The corpus callosum was the second most common area involved in diffuse axonal injury (21.5% of lesions). The vast majority (71.9%) of callosal lesions were found in the splenium (Fig. 2). Although the splenial lesions were usually unilateral and slightly eccentric to the midline, in several instances involvement was bilateral. These lesions were most clearly imaged on highly T1-weighted (inversion-recovery or spin-echo) axial scans. There was a very strong association be-

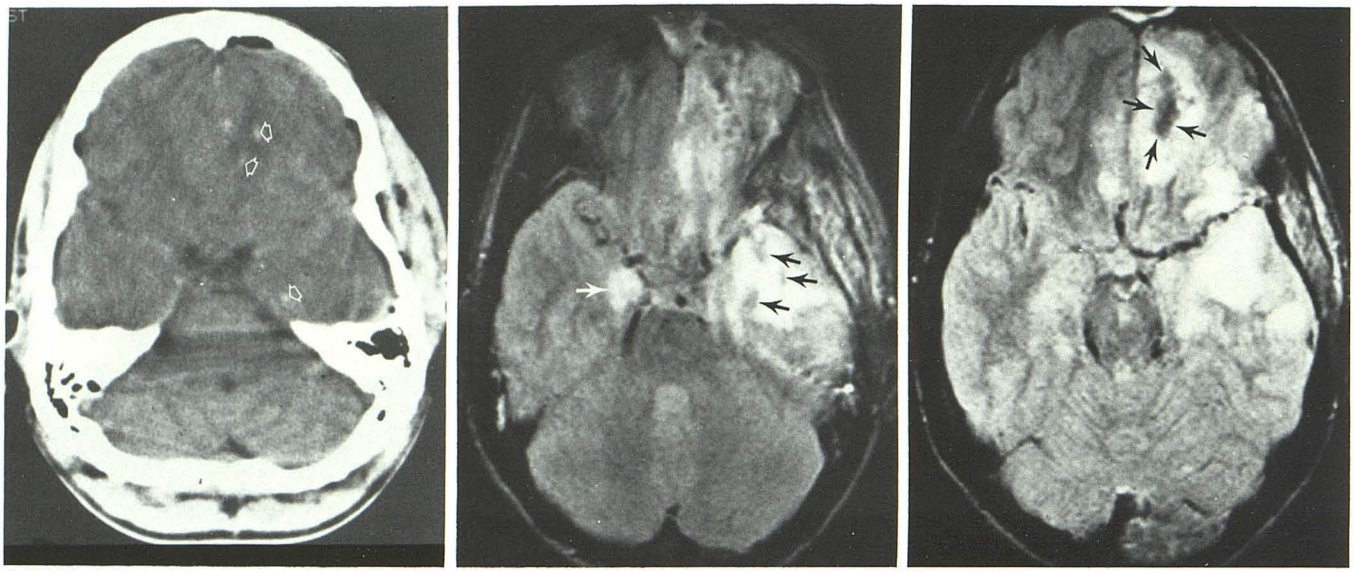

Fig. 3.—18-year-old man.

***A*, Axial CT scan the day of trauma appears essentially normal except for small petechial hemorrhages (*arrows*) in medial temporal and inferior frontal lobes. Note slight medial displacement of uncus of left temporal lobe.**

***B* and *C*, Axial T2-weighted spin-echo scans (TR = 2300 msec, TE = 80 msec) 5 days after trauma. Areas of abnormality (hemorrhagic contusions) are much more extensive on MR. Hemorrhagic areas (*black arrows*) are surrounded by much larger regions of nonhemorrhagic injury. Lesion in right temporal uncus (*white arrow*) could either represent primary cortical contusion or be secondary to pressure necrosis from transtentorial herniation.**

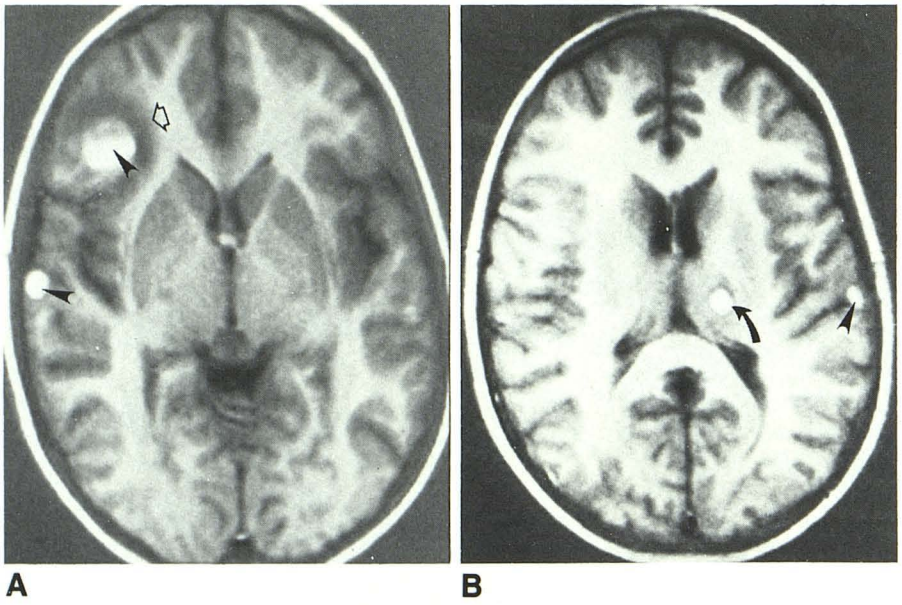

Fig. 4.—15-year-old girl. Axial T1-weighted inversion-recovery (TR = 2100 msec, TI = 600 msec) MR images 6 days after trauma show multiple hemorrhagic cortical contusions along inferolateral aspects of frontal and temporal lobes (*arrowheads*). Hemorrhagic nature of contusions is evident by short T1 of methemoglobin within hematomas. Peripheral nonhemorrhagic zone of injury and edema (*open arrow*) is hypointense because of its long T1. Note hemorrhagic subcortical gray-matter lesion in thalamus (*curved arrow*). This type of lesion may result from shear-strain disruption of perforating blood vessels.

tween the presence of corpus callosum lesions and intraventricular hemorrhage (IVH). While only 8.7% of the 23 patients without callosal lesions had IVH, 52.9% of the 17 patients with callosal lesions demonstrated IVH. The sizes of diffuse axonal lesions in the corpus callosum were usually larger than those in other locations.

Of the diffuse axonal lesions, 18.8% were located in the corona radiata, with slightly more than half in its posterior portion. These were usually slightly larger than those located more superficially in the lobar white matter. Only 8.1% of diffuse axonal lesions were in the capsular region, with most of these involving the posterior limb of the internal capsule. Most internal capsule lesions were found at its junction with the cerebral peduncle.

Cortical Contusions

The second most common type of traumatic lesion was the cortical contusion [13, 16, 17, 24–30]. To be placed in this category, the lesion had to (1) primarily involve the superficial cortex; (2) show relative sparing of the underlying white matter; (3) have a dural or osseous base; and (4) have a

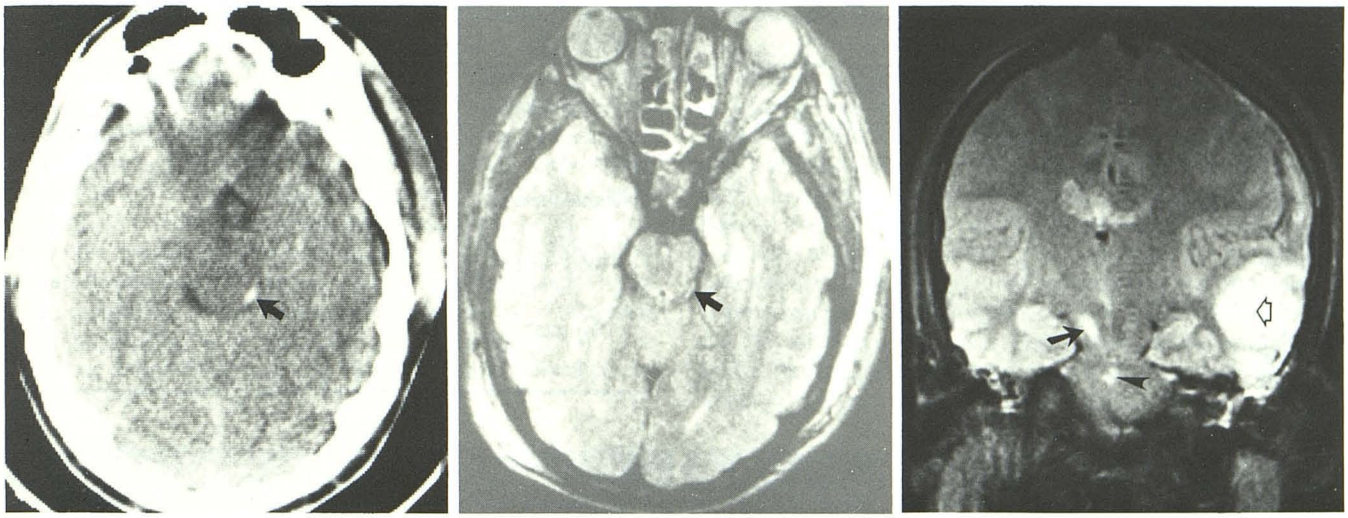

Fig. 5.—Primary brainstem injury.

***A* and *B*, Axial CT scan the day of trauma (*A*) and T1-weighted spin-echo MR image (TR = 1000 msec, TE = 40 msec) 2 days after trauma (*B*) in 21-year-old man. Lesion in dorsolateral aspect of midbrain (*arrows*) is typical in location for primary brainstem injury. Although lesion is clearly seen on CT scan it was seen on MR only retrospectively.**

***C*, Coronal T2-weighted MR image (TR = 2300 msec, TE = 80 msec) 5 days after trauma reveals central area of abnormality in pons (*arrowhead*) and large traumatic lesion in right cerebral peduncle (*solid arrow*). Also noted is large cortical contusion in lateral aspect of temporal lobe (*open arrow*).**

TABLE 2: Diffuse Axonal Injury—Frequency and Distribution of Lesions

Location	No. of Lesions		
	Hemorrhagic	Nonhemorrhagic	Total
Corona radiata (n = 28):			
Anterior	1	11	12
Posterior	2	14	16
Corpus callosum (n = 32):			
Genu	0	3	3
Body	4	2	6
Splenium	2	21	23
Capsule (n = 12):			
Internal	2	7	9
External	1	2	3
Lobar white matter (n = 71):			
Frontal	8	28	36
Temporal	4	19	23
Parietal	2	5	7
Occipital	0	5	5
Cerebellum (n = 4)	1	3	4
Other (n = 2)	1	1	2
Total	28	121	149

shape, character, and anatomic distribution not compatible with an infarct. Cortical contusions represented 43.7% of all primary lesions (Table 3) (Figs. 1–5). Cortical contusions also tended to be multiple, with 54.8% of lesions found in 20% of the study patients. Unlike diffuse axonal injury, cortical contusions were less likely to be associated with severe initial impairment of consciousness, as measured by the admission GCS scores. A much higher percentage of cortical contusions (51.9%) were hemorrhagic than were diffuse axonal injury lesions (18.8%). This may reflect the greater vascularity of gray matter. The hemorrhagic foci tended to be multiple, irregular, often confluent regions found within larger nonhemorrhagic zones of injury (Figs. 1, 3, and 4). Hemorrhagic lesions were more often distributed along the inferolateral surfaces of the frontal and temporal lobes (Table 3).

The temporal lobe was the most common site of cortical contusions (45.9% of lesions). Although the lateral aspect of the temporal lobe was the region most often injured, a significant percentage of lesions was also found along the medial surface and anterior pole. In this series, only 9.7% of temporal-lobe contusions primarily involved the inferior surface. The frontal lobe was the second most common site for contusions (31.1% of lesions). The vast majority of these lesions were found along the lateral aspect of this lobe or in a subfrontal location just above the lesser sphenoid wing and planum sphenoidale. The frontal pole was seldom involved.

The parietooccipital lobes and cerebellum were the sites of 13.3% and 9.6% of cortical contusions, respectively. Those in the parietooccipital region were most prevalent along the lateral convexity. Cerebellar lesions typically involved the superior vermis, tonsils, and inferior aspects of the hemispheres.

Subcortical Gray-Matter Lesions

Fourteen traumatic lesions were localized to the subcortical gray matter, representing only 4.5% of all primary lesions (Fig. 4). A higher percentage of these lesions (57.1%) were hemorrhagic as compared with any other type of lesion. This is most likely due to the high vascularity of this portion of the brain, supplied by a rich network of perforating vessels. The majority of these lesions were confined to the thalamus (Table 4). The severity of neurologic impairment for the eight patients with this type of injury was greater (mean GCS = 7.6) than that for all patients in this series (mean GCS = 9.8). The mechanism for production of this type of lesion may be the same as that for a similar category of lesions described by

TABLE 3: Cortical Contusion—Frequency and Distribution of Lesions

Location	No. of Lesions		
	Hemorrhagic	Nonhemorrhagic	Total
Frontal lobe (n = 42):			
Inferior	14	6	20
Superior	3	0	3
Medial	1	2	3
Lateral	10	3	13
Pole	1	2	3
Temporal lobe (n = 62):			
Inferior	5	1	6
Medial	5	13	18
Lateral	10	13	23
Pole	6	9	15
Parietooccipital (n = 18):			
Medial	3	1	4
Lateral	6	5	11
Superior	2	1	3
Cerebellum (n = 13):			
Hemisphere	3	5	8
Vermis	1	4	5
Total	70	65	135

TABLE 4: Subcortical Gray-Matter Lesions—Frequency and Distribution

Location	No. of Patients		
	Hemorrhagic	Nonhemorrhagic	Total
Thalamus	6	3	9
Caudate nucleus	0	0	0
Lentiform nucleus:			
Globus pallidus	2	0	2
Putamen	0	3	3
Subtotal	2	3	5
Total	8	6	14

TABLE 5: Brainstem Lesions—Frequency and Distribution of Lesions

Location	No. of Patients		
	Hemorrhagic	Nonhemorrhagic	Total
Midbrain:			
Tectum	0	1	1
Lateral tegmentum	1	1	2
Ventral tegmentum	0	1	1
Cerebral peduncle	0	1	1
Subtotal	1	4	5
Pons	1	3	4
Medulla	0	2	2
Total	2	9	11

Adams et al. [11, 27, 28]. They described a diffuse type of injury characterized by multiple petechial hemorrhages primarily located in the ventral brainstem, basal ganglia, and frontotemporal white matter. These lesions are most often seen in severely injured patients who die shortly after head injury. It was postulated by Adams et al., and consistent with the predictions of Holbourn [24, 25], that this form of injury may be secondary to disruption of multiple small perforating blood vessels (Fig. 4B).

Primary Brainstem Lesions

Ten patients (11 lesions) were thought to have lesions of the brainstem (Table 5) (Fig. 5) that were believed to have been caused by the initial traumatic force [12, 26–28, 31–33]. This group of patients generally had multiple other lesions, most of which were typical of diffuse axonal injury. Only two (18.2%) of the brainstem lesions were hemorrhagic. The severity of initial impairment of consciousness in this group of patients was greater than that for any other group. The mean initial GCS for these patients was 7.0. Five patients had focal neurologic findings that were anatomically compatible with the lesion imaged by MR. The other five patients had altered levels of consciousness but no focal neurologic findings. The majority of primary brainstem lesions (six of 11) were localized to the dorsal and lateral aspects of the rostral brainstem (midbrain and rostral pons) (Table 5). These lesions are most likely from diffuse axonal injury of the brainstem secondary to rotationally induced shear strains [26–28].

Classification, Characterization, and Localization of Secondary Brain Injury

Although the thrust of this article is concerned with primary forms of injury, we did observe several instances of secondary forms of injury that must be differentiated from primary lesions (Table 1). A number of excellent pathologic reports have dealt with the differentiation of primary and secondary forms of injury [11, 13, 17, 26–33]. Pressure necrosis, commonly associated with increased intracranial pressure and brain herniation syndromes, typically results when neural structures are compressed against rigid osseous and dural margins. This most commonly involved the cingulate (n = 5) and parahippocampal (n = 7) gyri in our series. It was often difficult to separate pressure necrosis from primary lesions (Fig. 3). The presence of significant mass effect, cisternal compression, and midline displacement often suggested pressure necrosis. Territorial arterial infarction was encountered in only one patient (Fig. 6). Diffuse hemispheric brain swelling and edema were not apparent in any patient as an isolated process, but were always associated with an underlying injury to the brain (cortical contusion, diffuse axonal injury, extraaxial hematoma, territorial infarction).

MR Imaging Plane and Pulse Sequences

The visibility of a lesion on a particular pulse sequence was influenced by a number of factors (presence of hemorrhage, interval of time since injury, size and anatomic location of the lesion). The overall relationships between lesion detectability and the presence of hemorrhage for various MR pulse sequences were examined in part 1 of this report [16]. The most important factor that affected lesion visibility was the MR imaging pulse sequence used. T2-weighted images were the

most sensitive over the whole course of injury (acute and subacute phases) and were similarly sensitive for hemorrhagic and nonhemorrhagic forms of injury. T1-weighted images were highly sensitive for hemorrhagic lesions, especially if the study was performed at least 3 days after injury. T1-weighted scans were less sensitive for nonhemorrhagic lesions and for very small (<1.0 cm) hemorrhagic lesions in the first 2 days after injury. T1-weighted images were slightly superior to T2-weighted images for the evaluation of the brainstem. This was primarily because small brainstem lesions were more often obscured on the T2-weighted scans by phase-shift artifacts arising from vascular and CSF pulsation. T2-weighted images were usually superior when these artifacts were absent.

The MR imaging plane was less important than the pulse sequence in lesion detectability (Table 6). The axial and coronal planes showed similar sensitivities for detecting all types of lesions. This was true for both T1- and T2-weighted pulse sequences. For specific lesions, however, one plane of imaging was often superior. The superficial lesions were seen best when the imaging plane was perpendicular to the cortical base of the lesion. Deep subcortical lesions were seen equally well with all imaging planes. The best plane for visibility of callosal lesions depended on the portion involved. Axial scans were superior for visualizing lesions in the genu and splenium (Fig. 2), while coronal scans were better for those within the body. Since brainstem lesions were usually small, multiple imaging planes were frequently helpful in detecting them.

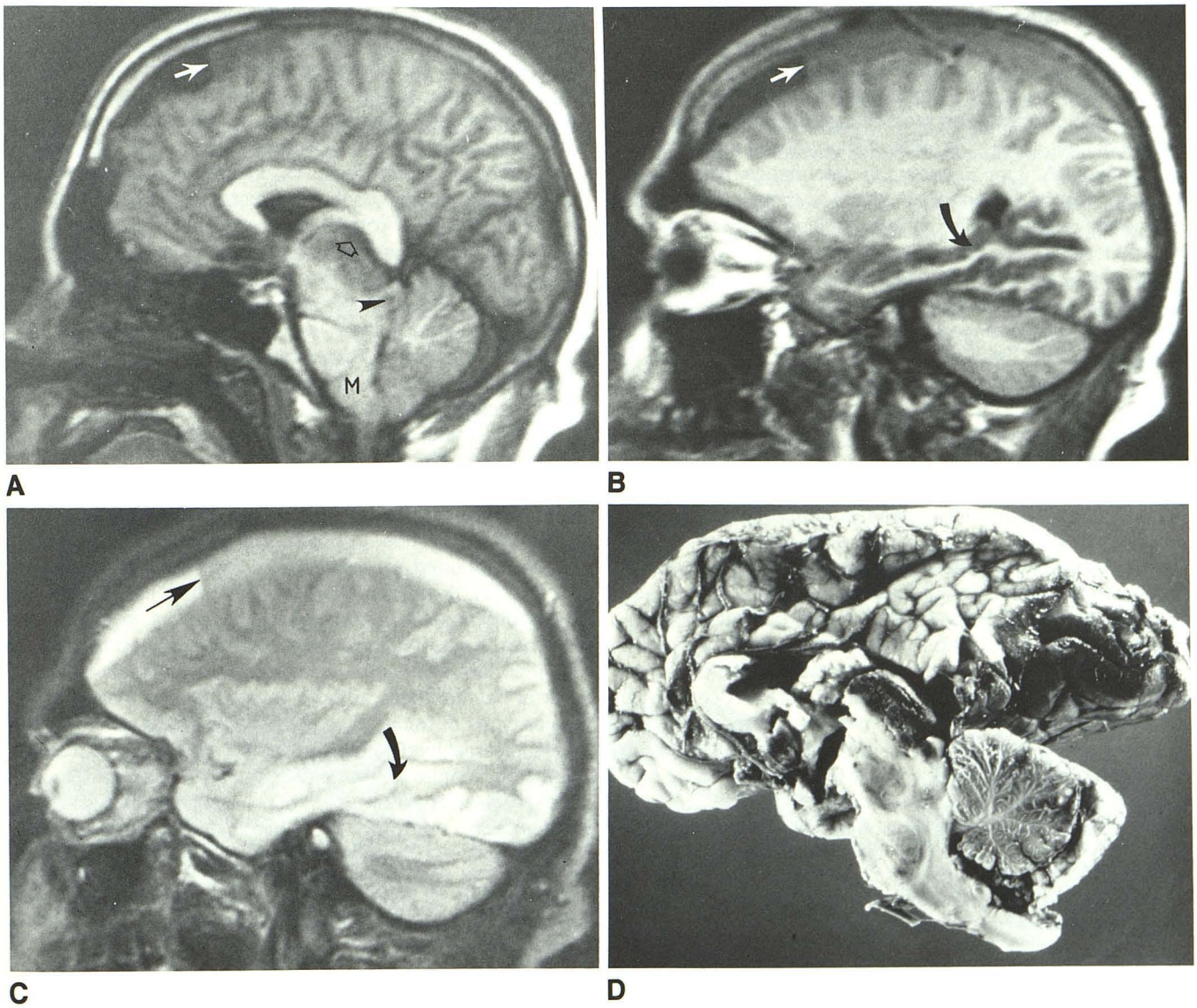

Fig. 6.—34-year-old comatose man who had several episodes of head trauma 1–3 weeks earlier.

***A–C*, Sagittal T1-weighted inversion-recovery (TR = 2350 msec, TE = 600 msec) MR images (*A* and *B*) and T2-weighted spin-echo (TR = 2300 msec, TE = 80 msec) MR image (*C*) show subdural hematoma with sedimentation level (*straight solid arrows*). There are areas of infarction in inferomedial temporal lobe (*curved arrows*) and thalamus (*open arrow*), respectively, in distributions of posterior cerebral and thalamoperforating arteries. There is evidence of transtentorial and tonsillar herniation. Note marked compression of midbrain (*arrowhead*), fourth ventricle, and interpeduncular cistern as well as kinking of medulla (M).**

***D*, Autopsy specimen. Lateral view of left half of brain after midsagittal section confirms MR findings.**

Multiple imaging planes were also helpful for classifying the type of traumatic lesion. For example, it was often difficult, with only one plane of imaging, to determine whether a small lesion close to the cortical surface was from diffuse axonal injury or cortical contusion. Only when the imaging plane was perpendicular to the adjacent calvarium was this reliably established (Fig. 1).

Discussion

Mechanisms of Cerebral Injury

Holbourn [24, 25] was the first to systematically analyze the mechanisms by which traumatic stresses produce cerebral injury. His experimental work, which used a gelatin model of the brain, has served as a fundamental basis for understanding the mechanisms of cerebral injury. He analyzed the mechanics of injury from a physicist's point of view and emphasized that injury to the brain could only occur through two types of structural deformations. *Compression-rarefaction strain* is characterized by a change in volume without a change of shape and is of minimal importance in the production of cerebral injury. *Shear-strain* deformation, however, is characterized by a change in shape without a change in volume and is responsible for the vast majority of mechanically induced lesions. The brain is relatively resistant to injury by compression-rarefaction strain because of its incompressibility. Brain tissue is quite susceptible, however, to shear-strain injury, since this depends on rigidity to prevent deformation. The brain, unlike the highly rigid skull, has a low index of rigidity and is ineffective in preventing this type of deformation [24, 25].

Holbourn also described two major types of forces responsible for brain deformation and injury. The first type of force is localized to the site of impact and is from skull distortion (contact phenomenon). These injuries are produced by localized inbending and fracture of the skull and are mediated through shear-strain distortions localized to the superficial regions of the brain. Compression-rarefaction strain waves do emanate from the site of impact but, according to Holbourn, they play little or no role in injury. The second group of forces includes those that arise irrespective of skull deformation (linear acceleration, rotational acceleration, centrifugal force, Coriolis force). Of the four forces in this group, rotational acceleration plays the predominant role in the production of intraaxial cerebral lesions [14, 24, 25]. Rotational forces produce traumatic lesions by deformation of brain tissue mediated through shear strains. The other three forces are much less important in the production of structural damage, either because the magnitude of the deforming force is small or because the force primarily exerts itself through deformations of the compression-rarefaction variety [13, 24–26].

Injuries from the shear-strains generated by rotational forces, as would be expected, are more diffuse in location than those from skull deformation. The expected anatomic distribution of traumatic lesions induced by nonimpact rotational acceleration was experimentally mapped by Holbourn [24, 25] with a gelatin brain model. Despite the limitation of this model, the location and distribution of traumatic lesions in fatal head injuries [11, 13–15, 17, 22, 23, 28] and animal trauma models [13, 26, 27] have generally followed Holbourn's theoretical predictions (Fig. 7). Injuries from rotational forces are expected to correspond closely in location to the sites of maximum shear-strain. Shear-strain will be greatest at the junction of tissues of different rigidity (gray/white-matter interface, brain/CSF interface, skull/brain interface, dura matter/brain interface) [24, 25]. The location of rotationally induced shear-strain lesions is primarily dependent on the plane of rotation (Fig. 7) and is independent of the direction of rotation within a given plane. The location of maximum shear-strain is also independent of the distance from the center of rotation, the arc of rotation, and the intensity of the force. The magnitude of shear-strain, however, is dependent on these factors as well as on the duration of the rotational force. Figure 7 illustrates the location of maximum shear-strain for all three orthogonal planes of rotation [24, 25]. Holbourn [24, 25] also emphasized that rotationally induced shear-strain deformations also act on nonneuronal tissue (penetrating blood vessels, bridging veins).

For a number of years Holbourn's classic work went ignored. Strich [22, 23] was the first to recognize the significance of Holbourn's observations with the publication of a pathologic description of shear injuries of the white matter. Since that time, most of Holbourn's observations have been largely supported by postmortem observations [11, 13–15, 17, 27, 28]. It was not until Gennarelli et al. [13, 21, 26, 27] developed an animal model of cranial trauma, however, that Holbourn's observations were confirmed experimentally. In an important series of experiments with a primate model of cranial trauma, these authors have confirmed that all of the major types of traumatic lesions can be reproduced by nonimpact inertial loading of the head in an appropriate manner. The exact nature of the resulting injury will depend on the type (angular, linear), rate, duration, and plane of head acceleration.

TABLE 6: Sensitivities of MR Imaging Planes in Detecting Primary Lesions

Type of Lesion	No. of Lesions Imaged/Total = % Sensitivity			
	Axial Plane		Coronal Plane	
	T1-Weighted	T2-Weighted	T1-Weighted	T2-Weighted
Diffuse axonal injury	71/90 = 78.9	140/149 = 94.0	40/58 = 69.0	59/67 = 88.1
Cortical contusions	60/81 = 74.1	127/135 = 94.1	38/51 = 74.5	65/70 = 92.9
Subcortical gray-matter lesions	9/10 = 90.0	13/14 = 92.9	3/5 = 60.0	8/8 = 100
Brainstem	7/9 = 77.8	7/11 = 63.6	2/3 = 66.8	4/7 = 57.1
Total	147/190 = 77.4	287/309 = 92.9	83/117 = 70.9	136/152 = 89.5

Classification and Distribution of Primary Traumatic Lesions

It is apparent from the studies of Holbourn [24, 25] that most intraaxial traumatic brain lesions result from either (1) skull deformation or fracture (contact phenomenon) or (2) nonimpact stresses related to rotational acceleration. Furthermore, these two types of mechanisms are primarily mediated through the same type of deformation (shear-strain). Since all traumatic lesions are produced by the same type of deformation and differ primarily by their location, it seems most valid to base their classification on the latter point. We believe the primary traumatic intraaxial lesions found in this study clearly fit into four anatomically well-defined categories: (1) diffuse axonal injury, (2) cortical contusion, (3) subcortical gray-matter injury, and (4) brainstem injury (Tables 2–5). This proposed classification scheme, based on the topographic and anatomic location of lesions, closely resembles that used by other authors [11, 13–17, 26–28, 32, 33]. We think that this simple method of classification is practical and applicable to both radiologic imaging and pathologic analysis. It also avoids imprecise nomenclature that may falsely imply mechanistic processes (for example, coup/contracoup/intermediary coup, contusion laceration, stretching contusion, gliding contusion) [11].

Previously, there has not been a satisfactory means for anatomically staging and classifying lesions in the living patient. The GCS has provided a clinical means for judging the severity of injury, making decisions about the need for intracranial pressure monitoring, determining the prognosis for recovery, and comparing responses to treatment. Accurate anatomic classification of traumatic lesions would also be potentially useful for similar reasons. It might also prove helpful for further clarifying the mechanisms of cerebral injury. Despite these potential benefits, CT has not been particularly useful for classifying and staging injury. Its low sensitivity for nonhemorrhagic lesions and the difficulty of obtaining multiplanar images have severely limited its usefulness [13, 16–18].

MR offers distinct advantages over other imaging methods for classifying traumatic cerebral lesions. The ability of MR to image in multiple planes is particularly beneficial since this makes lesion localization much easier (Fig. 1). Unless two planes of imaging are used, it is often difficult to differentiate a diffuse axonal injury lesion involving the gray/white-matter interface from a small cortical contusion. In addition, more lesions can be classified with MR than with CT because MR has a much higher sensitivity for nonhemorrhagic lesions (Fig. 3) [16].

We believe there is little difficulty, with this classification scheme, in separating the various types of primary lesions, since the anatomic location of each type of lesion is distinctive. We did experience some difficulty in distinguishing primary and secondary lesions, since both types are often found in the same locations (Fig. 3). This problem, however, is not unique to MR, as it may also be difficult to make this distinction at autopsy or on a histologic basis [11–15, 27–33]. Despite these problems, we believe that in most cases a distinction can be made with MR on the basis of the size, shape, distribution, and location of the lesions. It is possible, however, that a number of lesions that we believed to be primary were actually secondary. Much experience is needed in closely correlating the MR and histologic appearances of lesions in various stages of evolution to accomplish this goal. Sequential MR scanning, beginning shortly after trauma, may be helpful.

An important limitation of the value of this prospective study is the lack of pathologic confirmation in the majority of our cases. Autopsy confirmation of the exact nature of the lesions was possible in only one patient, since 39 of 40 patients survived their injuries. Despite this limitation, we believe that, for the first time in the living patient, it is possible to detect and classify most types of traumatic injuries with MR. A comparison of the anatomic distribution of the lesions in our group of patients with that from pathologic [13–15, 17, 22, 23, 28] and animal studies [13, 26, 27] reveals an identical overall pattern. The pattern of lesions seen in our patients (Tables 2–5) is also remarkably similar to the theoretical predictions of Holbourn [24, 25] (Fig. 1). The similarity in the patterns would suggest that MR does detect the full spectrum of lesions.

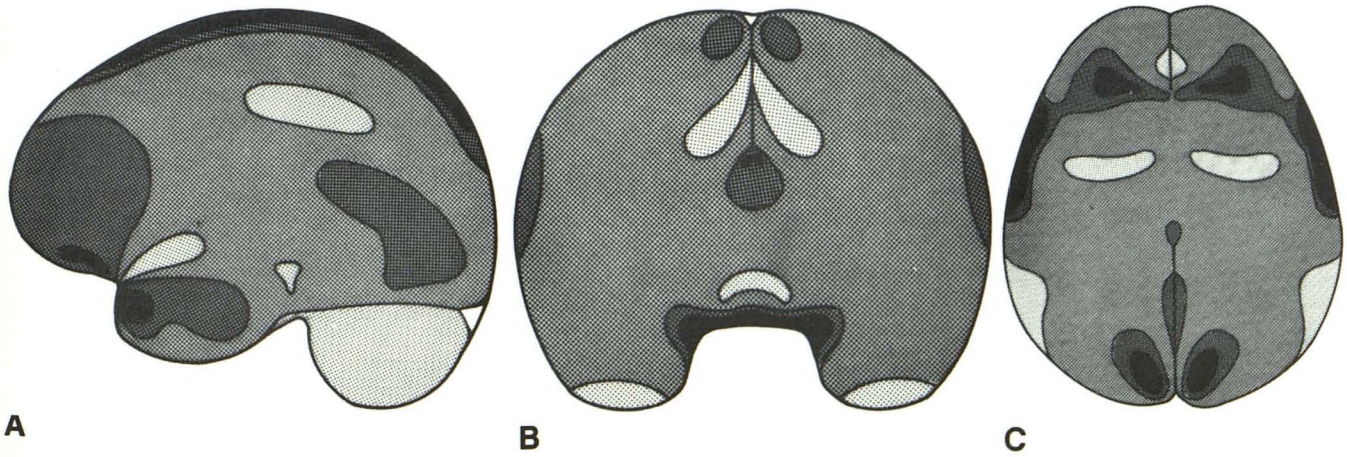

Fig. 7.—Areas of maximum shear-strain and predicted distribution of traumatic intraaxial lesions for three orthogonal planes of rotational acceleration. Expected location of traumatic lesions for rotation in sagittal (*A*), coronal (*B*), and axial (*C*) planes. Greater frequency of lesions is to be anticipated in more darkly shaded regions, which represent areas of maximum shear-strain. (Adapted from [24].)

MR Imaging Plane and Pulse Sequences

We believe that is is essential to obtain images that emphasize both T1 and T2 contrast differences in at least two different imaging planes to accurately detect, characterize, and classify traumatic lesions [16]. Generally speaking, T2-weighted images are most useful for lesion detection, both types of images are necessary for accurate detection and temporal staging of hemorrhagic lesions [20], and T1-weighted images are most useful for anatomically localizing the lesions for purposes of classification. The protocol that we find most practical for our particular scanner is as follows: (1) Sagittal T1-weighted images (short TR, short TE spin-echo scans) are initially obtained, the images of which are used to plan the imaging planes for the other pulse sequences; (2) an axial T2-weighted (long TR, long TE spin-echo) study is then performed. If no abnormalities are seen on the first two sequences the examination is stopped. If traumatic lesions are visualized, then the study also includes (3) coronal T1-weighted images with either an inversion-recovery or short TR, short TE spin-echo sequence through regions of pathology.

REFERENCES

1. Zimmerman RD, Danziger A. Extracerebral trauma. *Radiol Clin North Am* **1982**;20:105–121
2. Hryshko FG, Deeb ZL. Computed tomography in acute head injuries. *J Comput Tomogr* **1983**;7:331–334
3. Zimmerman RA, Bilaniuk LT, Gennarelli T. Computed tomography of shearing injuries of the cerebral white matter. *Radiology* **1978**;127:393–396
4. Zimmerman RA, Bilaniuk LT, Bruce D, Dolinskas C, Obrist W, Kuhl D. Computed tomography of pediatric head trauma: acute general cerebral swelling. *Radiology* **1978**;126:403–408
5. French BN, Dublin AB. The value of computerized tomography in the management of 1000 consecutive head injuries. *Surg Neurol* **1977**;7:171–183
6. Moseley IF, Zilkha E. The role of computerized axial tomography (EMI-scanning) in the diagnosis and management of craniocerebral trauma. *J Neuroradiol* **1976**;3:277–296
7. Bricolo A, Pasut MI. Extradural hematoma toward zero mortality. A prospective study. *Neurosurgery* **1984**;14:8–12
8. Seelig JM, Becker DP, Miller JD, Greenberg RP, Ward JD, Choi SC. Traumatic acute subdural hematoma. Major mortality reduction in comatose patients treated within four hours. *N Engl J Med* **1981**;304:1511–1518
9. Lanksch W, Grumme T, Kazner E. Correlations between clinical symptoms and computerized tomography findings in closed head injuries. In: Frowein RS, Wilcke D, Karimi-Nejad A, Brock M, Klinger M, eds. *Advances in neurosurgery*, vol 5. *Head injuries—tumors of the cerebellar region*. Berlin: Springer-Verlag, **1978**:27–29
10. Snoek J, Jennett B, Adams JH, Graham DI, Doyle D. Computerized tomography after recent severe head injury in patients without acute intracranial hematoma. *J Neurol Neurosurg Psychiatry* **1979**;42:215–225
11. Adams JH, Graham DI, Scott G, Parker LS, Doyle D. Brain damage in fatal non-missile head injury. *J Clin Pathol* **1980**;33:1132–1145
12. Cooper PR, Maravilla K, Kirkpatrick J, et al. Traumatically induced brainstem hemorrhage and the computerized tomographic scan: clinical, pathological and experimental observations. *Neurosurgery* **1979**;4:115–124
13. Adams JH, Gennarelli TA, Graham DI. Brain damage in non-missile head injury: observations in man and subhuman primates. In: Smith WT, Cavanagh JB, eds. *Recent advances in neuropathology*, vol 2. Edinburgh: Churchill Livingston, **1982**:165–190
14. Adams JH, Graham DI, Murray LS, Scott G. Diffuse axonal injury due to non-missile head injury in humans: an analysis of 45 cases. *Ann Neurol* **1982**;12:557–563
15. Adams JH, Mitchell DE, Graham DI, Doyle D. Diffuse brain damage of immediate impact type: its relationship to primary brainstem damage in head injury. *Brain* **1977**;100:489–502
16. Gentry LR, Godersky JC, Thompson B, Dunn VD. Prospective comparative study of intermediate-field MR and CT in the evaluation of closed head trauma. *AJNR* **1988**;9:91–100
17. Hardman JM. The pathology of traumatic brain injuries. *Adv Neurol* **1979**;22:15–50
18. Perini S, Beltramello A, Pasut ML, Benati A, Bricolo A. CNS trauma: head injuries. *Neurol Clin* **1984**;2:719–743
19. Dunn VD, Ely-Coffman C, McGowan JE, Ehrhardt JC. Mechanical ventilation during magnetic resonance imaging. *Magnetic Resonance Imag* **1985**;3:169–172
20. Gomori JM, Grossman RI, Goldberg HI, Zimmerman RA, Bilaniuk LT. Intracranial hematomas: imaging by high field MR. *Radiology* **1985**;157:87–93
21. Gennarelli TA, Spielman GM, Langfitt TW, et al. Influence of the type of intracranial lesion on outcome from severe head injury. *J Neurosurg* **1982**;56:26–32
22. Strich SJ. Diffuse degeneration of the cerebral white matter in severe dementia following head injury. *J Neurol Neurosurg Psychiatry* **1956**;19:163–185
23. Strich SJ. Shearing of nerve fibers as a cause of brain damage due to head injury, a pathological study of twenty cases. *Lancet* **1961**;2:443–448
24. Holbourn AHS. Mechanics of head injuries. *Lancet* **1943**;2:438–441
25. Holbourn AHS. The mechanics of brain injuries. *Br Med Bull* **1945**;3:147–149
26. Gennarelli TA, Thibault LE, Adams JH, Graham DI, Thompson CJ, Marcincin RP. Diffuse axonal injury and traumatic coma in the primate. In: Dacey RG Jr, Winn HR, Rimel RW, Jane JA, eds. *Trauma of the central nervous system*. New York: Raven, **1985**:169–193
27. Adams JH, Graham DI, Gennarelli TA. Contemporary neuropathological considerations regarding brain damage in head injury. In: Becker DP, Polishock J, eds. *Central nervous system trauma status report*. Bethesda, MD: National Institute Neurological and Communicative Disorders and Stroke, National Institute of Health. **1985**:65–77
28. Adams JH. Head injury. In: Adams JH, Corsellis JAN, Duchen LW, eds. *Greenfield's neuropathology*, 4th ed. New York: Wiley, **1984**:85–124
29. Lindenberg R, Freytag E. The mechanism of cerebral contusions: a pathologic-anatomic study. *Arch Pathol Lab Med* **1960**;69:440–469
30. Lindenberg R, Fisher RS, Durlacher SH, Lovitt WV Jr, Freytag E. Lesions of the corpus callosum following blunt mechanical trauma to the head. *Am J Pathol* **1955**;31:297–317
31. Rosenblum WI, Greenberg RP, Seelig JM, Becker DP. Midbrain lesions: frequent and significant prognostic feature in closed head injury. *Neurosurgery* **1981**;9:613–620
32. Tomlinson BE. Brainstem lesions after head injury. *J Clin Pathol [Suppl]* (R Coll Pathol) **1970**;4:154–165
33. Tsai FY, Teal JS, Quinn MF, et al. CT of brainstem injury. *AJNR* **1980**;1:23–29, *AJR* **1980**;134:717–723